Risk mitigation for application of Li-ion batteries on submarines by modelling of heat and combustible gasses development during a thermal runaway

T. H. Wien, LTZ3[a], ir. N. H. D. Gartner[b*], dr. ir. R. D. Geertsma, CEng, MIMarEST[a], prof. dr. ir. R. G. van de Ketterij[a]

[a]Netherlands Defence Academy, The Netherlands,[b] Defence Materiel Organisation, The Netherlands
*Corresponding author. Email: NHD.Gartner@mindef.nl

Synopsis

Submarines face an ongoing technical battle to improve the operational effectiveness by increasing the submerged endurance and range. Currently, diesel-electric submarines mostly implement traditional lead-acid batteries as the main source of power when submerged. Installing more modern battery systems, like lithium-ion batteries, on new or refitted diesel-electric submarines can increase the submerged range with up to a factor 2. Additionally, lithium-ion batteries require less maintenance and provide a relatively longer life expectancy compared to lead-acid batteries. However, lithium-ion batteries can develop a thermal runaway: a process which exponentially generates heat, leading to the risk of an explosion and fire. Additionally, the gasses formed in the thermal runaway process are toxic, corrosive and flammable. Therefore, research is required into preventing a thermal runaway of lithium-ion batteries and mitigating the risks caused by a thermal runaway on submarines. This paper investigates: a) the required cooling to prevent thermal runaway or limit it to a single cell, and, b) measures to protect crew and submarine against the consequences of a thermal runaway of lithium-ion batteries. The paper proposes and verifies a novel thermal runaway model based on a heat development model in literature and extends it with a model that establishes the quantity of released gasses. The modelling results demonstrate that it is essential to limit thermal runaway to a single cell and prevent propagation from cell-to-cell. This can be achieved by providing cooling with compressed air foam, thus cooling the neighbouring cells and containing the heat and combustible gasses within the battery compartment. In order to validate the results of this first conceptual investigation, further work is required to provide more detail to the evaluated protection measures and system designs by validating the thermal runaway models and validating the ultimate battery and protection systems supported by physical destructive tests.

Keywords: Lithium-ion batteries; Thermal runaway; Submarines; Safety; Modelling

1 Introduction

In the Defence Whitepaper 2022, the Netherlands Ministry of Defence announces it will invest in strengthening its specialisms in response to the reducing security and stability in the world (Netherlands Ministry of Defence, 2012). In these specialisms, future submarines play an important role in covertly gathering intelligence, supporting special forces operations from under water and being capable of launching long distance precision weapons for integrated air and missile defence. For these specialisms, future submarines require operational agility, which is mainly determined by its underwater range (Stapersma and Prins, 2020). Nuclear propulsion is not financially viable for future submarines for the Royal Netherlands Navy and fully battery electric submarines as proposed in De Vos et al. (2020) will not have sufficient range to operate worldwide. Therefore, the future submarine will be fitted with electric propulsion, supplied from a hybrid power supply, with a combination of batteries, air independent power sources such as a Stirling engine or fuel cell, and diesel generators (Geertsma et al., 2017). The main limitation of current air independent power sources is their limited power levels, which strongly limits the submerged speed and therefore the operational agility. Moreover, it is not expected that future fuel cell technologies will provide a breakthrough in this limitation (Stapersma and Prins, 2020). However, the increase in energy density of Li-ion batteries and its reduced maintenance requirement (Pilat et al., 2017), providing up to a factor 2 of submerged range, might prove to be a game changer for the operational agility of future submarines, if sufficient packing density can be achieved (Prins and Stapersma, 2020).

Authors' Biographies

sub-Lt (E) Tom Wien is a Naval Officer graduated at the Netherlands Defence Academy for a BSc. in Military Systems and Technology with his thesis on thermal runaway in lithium-ion batteries. He now studies for an MSc. in mechanical engineering at Delft University of Technology.

Ir. Niels Gartner is a marine engineer working at the Defence Materiel Organisation, responsible for battery systems and HVAC systems. He graduated for his MSc. Marine technology in 2021 with his thesis on the thermal behaviour of lithium-ion batteries and the implications on submarine system design.

Cdr (E) Rinze Geertsma currently is assistant professor at the Netherlands Defence Academy and guest researcher at Delft University of Technology with a research interest in sustainable and maintainable energy systems for ships. He has been Marine Engineering Officer of *HNLMS de Ruyter* and *HNLMS Tromp*. Earlier experience includes system and project engineering and in service support.

Prof. dr. ir. Robert van de Ketterij is currently the chair of the section Military Technology and Sciences at the Netherlands Defence Academy and responsible for research and development in the field of systems engineering. Earlier experience includes the managing director of Royal IHC - MTI Holland B.V., responsible for the Knowledge Centre regarding dredging, mining and deep-sea mining processes.

While the energy density of Li-ion provides exceptional operational advantages, Li-ion batteries provide an inherent safety risk, due to their high amount of stored energy and the risk of a thermal runaway (TR) that can be caused by a temperature rise in the battery (Wien, 2022; Gartner, 2021). As a result of a thermal runaway, the battery can ignite and explode. For an electric vehicle, the consequences of TR can be limited by placing the vehicle on the side of road and letting the vehicle burn out, and for surface ships, the risk is mitigated by ensuring venting channels to vent-off hot gasses and prevent propagation of TR from one module to another module of the battery system. However, on a submarine it is not easy to vent-off hot gasses and deal with the released energy from a TR while submerged, without affecting the safety of the crew. Therefore, new safety concepts are required for submarines to mitigate the risk of TR, to prevent module to module propagation of TR and to prevent that TR causes a risk to the safety of the crew on board a submarine and the continuation of its mission.

Due to the high safety risk of thermal runaway and the wide use of Li-ion batteries, in applications ranging from consumer electronics, through electric and hybrid vehicles to more recently ships, extensive research is performed in the mechanisms, modelling, detection and prevention of thermal runaway in Li-ion batteries, as demonstrated by the extensive review in Lai et al. (2021) and on the review on safety strategies for electric vehicles by Chombo and Laoonual (2020). However, the evaluation of safe application of Li-ion batteries on ships is rarely studied, although Rao et al. (2015) evaluated fire safety measures on lithium-ion battery systems for ships by performing fire tests with carbon dioxide, superfine powder and a gas based fire extinguishing system test. They conclude that the gas based fire extinguishing system using heprafluorpropane extinguishes the fire, which is partly attributed to the cooling effect of the evaporation of the liquid agent, thus reducing the temperature and limiting further reactions in the battery system. Similarly, Quintiere (2022) found that packaging of a water saturated sponge for multiple cylindrical consumer batteries could limit temperature rise by the boiling effect of water, thus preventing runaway propagation from cell to cell as it reduced the cell temperature to 230-330 °C and the surface temperature of the sponge packaging to approximately the boiling temperature of water, 100 °C. These works demonstrates the need for cooling and the effectiveness of (boiling) water as a cooling medium for Li-ion battery fires.

Thermal runaway modelling focuses on the heat and temperature development (Feng et al., 2015) and on the development of combustible gasses, that can cause explosion and further energy release (Golubkov et al., 2014; Koch et al., 2018). The heat and temperature development models can be used to analyse initiation and propagation of thermal runaway in standard EV-ARC tests, in which thermal runaway is initiated by heating the batteries or in punctures tests, in which thermal runaway is caused by creating a internal short circuit by puncturing the cell (Feng et al., 2015). The latter is representative for the worst case scenario and also is representative for thermal runaway due to production faults and mechanical, thermal or electrical abuse of Li-on batteries (Chombo and Laoonual, 2020). The gas analysis models are used to determine the amount of combustible gases that develop during thermal runaway with an autoclave setup, in which gasses are captured in a gas tight cylinder (Golubkov et al., 2014; Koch et al., 2018). These gases can lead to further explosions and energy release and to pressure build-up, in particular when not vented. The safety risks of Li-ion batteries in submarines focus on both heat development and on combustible gasses, as both heat and gasses cannot be easily mitigated on a submarine, thus the above mentioned modelling strategies need to be combined.

1.1 Aim and contribution

This paper investigates: a) the required cooling to prevent thermal runaway or isolate it to a single cell, and, b) measures to protect crew and submarine against the consequences of a thermal runaway of lithium-ion batteries. The paper proposes a novel thermal runaway model based on a heat development model in literature and extends it with a model that establishes the quantity of released gasses (reactants). This model is verified with results from literature and subsequently used to investigate the process of thermal runaway under a number of scenarios. In the investigated scenarios the modelling results demonstrate how much cooling is required to prevent a thermal runaway or limit it to a single cell and the effect of a fire extinguishing systems to limit the consequences of a thermal runaway and prevent cell-to-cell or module-to-module propagation. With the proposed modelling strategy, we gain more insight into the consequences of a TR and we can design and evaluate safety measures to maintain the safety of the submarine and its crew when implementing Li-ion batteries.

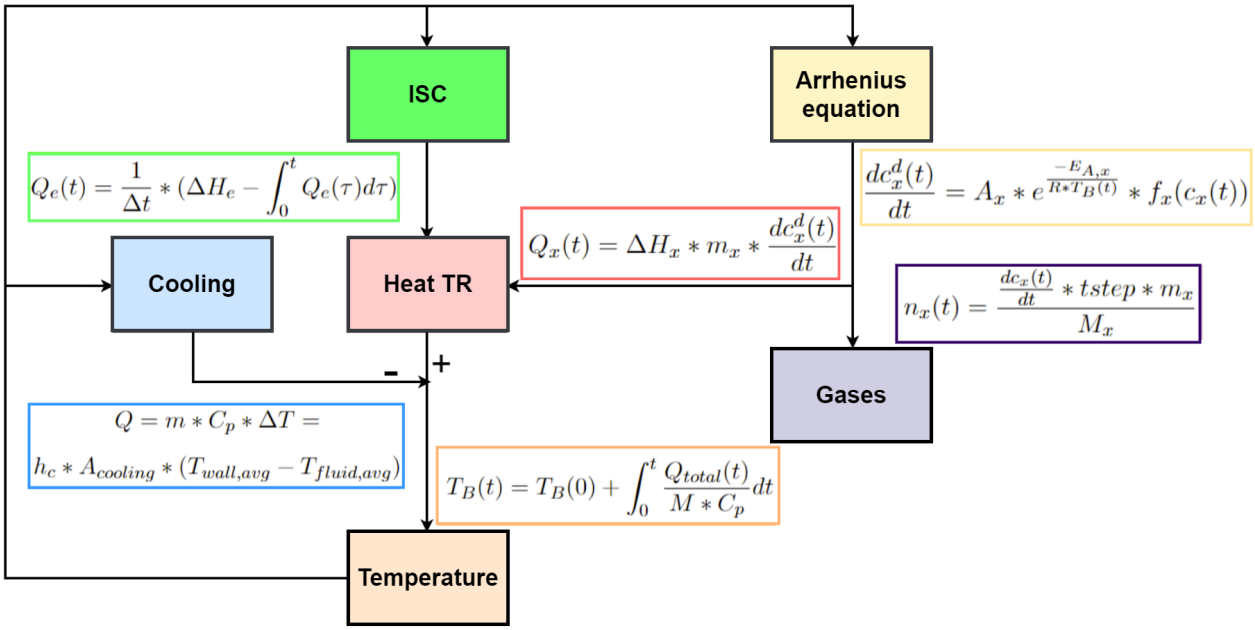

Figure 1: Schematic presentation of the created thermal runaway model.

2 Model description

In order to establish both the development of heat and released gasses during thermal runaway of a typical submarine battery, a model was developed for a single battery cell. The schematic representation of the model is illustrated in Figure 1. This model is partially based on the thermal model used in Feng et al. (2015) and also uses its parameters. The model starts when the temperature of the battery is equal to the onset temperature of the TR. The amount of heat and gas produced by a TR is determined by the rate at which the different reactions in the different phases of the TR take place. This rate can be determined using the Arrhenius equation. With this equation a concentration change can be calculated which can determine how much gas and heat per reaction is released. In addition to the heat caused by the concentration change, heat can also be released from an internal short circuit (ISC), but this only happens when the onset temperature of the ISC is reached. The heat can be fully or partially dissipated by cooling. If the cooling is insufficient, the temperature of the battery will rise and the rate of the reactions will change. Also other type of reactions may occur, especially if the increasing temperature leads to a new phase of the TR.

2.1 Temperature model

The temperature of the battery during thermal runaway can be established with Equation (1):

$$T_B(t) = T_B(0) + \int_0^t \frac{Q_{total}(t)}{M \cdot C_p} dt, \tag{1}$$

where the temperature $T_B(t)$ in K is a function of the total generated heat $Q_{total}(t)$ in W, mass M in g and the specific heat capacity C_p in $J/(g \cdot K)$. The total generated heat is the combined heat that is generated by all phases of the thermal runaway. The mass and specific heat capacity are values belonging to a specific battery (Feng et al., 2015). Not only does the temperature provide information about the battery's condition, but the temperature also influences which reactions take place and at which rate.

2.2 Heat generation model

In the heat generation model, two components add heat to the battery. As can be seen in Figure 1, those two components are the Arrhenius equation and the internal short circuit (ISC). The Arrhenius equation can be used to describe the rate at which the chemical reactions take place. The ISC is an electrical reaction happening inside the battery once the separator has melted and is responsible for the largest energy release during the TR.

2.2.1 Arrhenius equation

During the TR, different chemical reactions take place at different phases of the TR. The chemical reactions can create heat and contribute to a rise in temperature. Therefore, the heat of each reaction must be established with Equation (2):

$$Q_x(t) = \Delta H_x \cdot m_x \cdot \frac{dc_x^d(t)}{dt}, \quad (T_B(t) > T_{onset,x}), \tag{2}$$

where x stands for the different type of reactions that can take place during the TR, T_{onset} applies to these reactions, which means that the specific reaction only occurs when the temperature of the battery is higher than this temperature, $Q_x(t)$ in J/s is the heat generation of a particular reaction at a particular time, ΔH_x in J/g is the enthalpy of the chemical reaction, m_x in g is the mass of the reacting substance in reaction x, and $\frac{dc_x^d(t)}{dt}$ in $1/s$ is the decomposition rate of the normalised concentration of the reactant in reaction x. This last parameter can be determined by the Arrhenius equation, as seen in Equation (3):

$$\frac{dc_x^d(t)}{dt} = A_x \cdot e^{\frac{-E_{A,x}}{R \cdot T_B(t)}} \cdot f_x(c_x(t)), \quad (T_B(t) > T_{onset,x}) \tag{3}$$

To use the Arrhenius equation for the different type of reactions, some parameters have to be known. Those parameters differ significantly between the different type of reactions and should be measured with experimental tests. The parameters in the Arrhenius equation are: the frequency factor A_x in $1/s$, the activation energy $E_{a,x}$ in J/mol, the molecular gas constant R in $J/(mol \cdot K)$ and the temperature of the battery $T_B(t)$ in K. $f(c_x(t))$ is the last parameter and can be calculated by using the Sestak-Berggren equation (Feng et al., 2015).

2.2.2 Internal short circuit

The second component that delivers heat to the battery is the ISC. The ISC will release a lot of energy in a short period of time starting from the instant the separator melts. To calculate the amount of heat generated by the ISC, $Q_e(t)$ in J, Equation (4) can be used.

$$Q_e(t) = \frac{1}{\Delta t} \cdot (\Delta H_e - \int_0^t Q_e(\tau) d\tau), \quad (T_B(t) > T_{onset,e}), \tag{4}$$

where ΔH_e is the total amount of energy released, which is the amount of electrical energy stored in the battery, and Δt is the duration of the ISC and during this time the total amount of electrical energy will be released. These parameters are therefore two constants in the function. The amount of stored electrical energy of a battery can be determined by the capacity of the battery multiplied by the nominal voltage. This calculation applies at a state of charge (SOC) of 100%, but at lower SOC less energy is stored in the battery. At a lower SOC, less energy will be released during an ISC, but the relationship between the amount of energy and the SOC is not linear. To determine this relationship, more research is needed (Feng et al., 2015).

2.3 Gas generation model

The Arrhenius equation also determines how much gas is produced during the TR, as illustrated in Figure 1. The equation describes the decomposition rate and when compensated with the regeneration rate ($\frac{dc_x^g(t)}{dt}$ in $1/s$) a concentration change rate can be determined. Using the concentration change rate $\frac{dc_x(t)}{dt}$ in $1/s$, we can establish the amount of gas in moles that is produced at a specific moment by a specific chemical reaction using Equation (5):

$$n_x(t) = \frac{\frac{dc_x(t)}{dt} \cdot t_{step} \cdot m_x}{M_x}. \tag{5}$$

In this equation m_x in g is the total mass of substance x at the start of the TR, M_x in g/mol is the molar mass of x and t_{step} in s is the time step used in the model. To determine the total amount of moles gas that react per substance, all values of $n_x(t)$ must be summed. The chemical reactions used in this gas generation model are described in Table 1. Different chemical reactions happen at different phases of a TR. These reactions are specifically selected for a nickel manganese cobalt (NMC) battery with an electrolyte containing ethylene carbonate (EC) and diethyl carbonate (DEC). The reactions shown depend on the materials in the battery and therefore differ between different types of lithium-ion batteries. Other types of solvents will result in other chemical reactions. To give a complete overview of all common batteries, extensive research is needed to find the material composition and determine specific chemical reactions for these battery types and solvents. As we do not know exactly the composition of the NMC battery, we have to take into account this selection of chemical reactions could be incomplete and more research is needed to provide certainty. However, as proof of principle the table provides sufficient detail.

Table 1: Reaction equations used in the gas generation model

Section	Reaction equations for NMC(EC,DEC)
SEI	$(CH_2OCO_2Li)_2 \xrightarrow{\Delta H} Li_2CO_3 + C_2H_4 + CO_2 + \frac{1}{2}O_2$
	$2\,Li + (CH_2OCO_2Li)_2 \xrightarrow{\Delta H} 2\,Li_2CO_3 + C_2H_4$
Anode (T $<$ 260 °C)	$2\,Li + C_3H_4O_3(EC) \longrightarrow Li_2CO_3 + C_2H_4$
	$2\,Li + C_5H_{10}O_3(DEC) + 2\,H_2 \longrightarrow Li_2CO_3 + 2\,CH_4 + C_2H_6$
Anode (T $\geq$ 260 °C)	$-CH_2-CF_2^- + Li \xrightarrow{\Delta H} LiF + -CH{=}CF^- + \frac{1}{2}H_2$
Electrolyte	$C_3H_4O_3(EC) \longrightarrow CO_2 + x$
	$C_5H_{10}O_3(DEC) \longrightarrow CO + x$
Cathode 1	$Mn_2O_4 \longrightarrow Mn_2O_3 + \frac{1}{2}O_2$
Cathode 2	$Ni_{0.8}Co_{0.2}O_2 \longrightarrow \frac{1}{3}Ni_{2.4}Co_{0.6}O_4 + \frac{1}{3}O_2$
Li_2CO_3	$Li_2CO_3 + 2\,HF \xrightarrow{\Delta H} 2\,LiF + CO_2 + H_2O$
$O_2 \longrightarrow CO_2$	$\frac{5}{2}O_2 + C_3H_4O_3(EC) \xrightarrow{\Delta H} 3CO_2 + 2\,H_2O$
	$6\,O_2 + C_5H_{10}O_3(DEC) \xrightarrow{\Delta H} 5\,CO_2 + 5\,H_2O$
$O_2 \longrightarrow CO$	$O_2 + C_3H_4O_3(EC) \xrightarrow{\Delta H} 3CO + 2\,H_2O$
	$3\,\frac{1}{2}O_2 + C_5H_{10}O_3(DEC) \xrightarrow{\Delta H} 5\,CO + 5\,H_2O$

2.4 Cooling model

The cooling model can be used to investigate the minimum cooling water flow that is required to provide sufficient cooling to prevent cell-to-cell propagation during a thermal runaway of a single cell, for example due to a cell malfunction. We assume the cells are water cooled and the module design is such that sufficient heat can be transferred to the cooling water. A schematic representation of a potential module arrangement is a cooling water channel in between individual cells, as shown in Figure 2. Alternative heat conduction paths can be arranged in cell designs. Therefore, the model only gives an indication of the required cooling capacity and does not intend to accurately represent actual battery or module design. The battery cells are stacked in a module pack side by side. The water flow will absorb heat generated by the TR and transport the heat to a heat exchanger. In this scenario forced convection is applied according to:

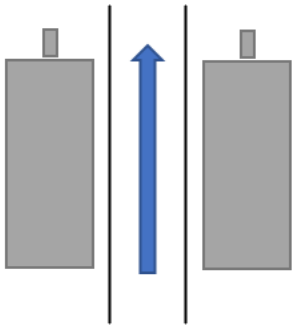

Figure 2: Schematic presentation of the cooling system.

$$Q = m \cdot C_p \cdot \Delta T = h_c \cdot A_{cooling} \cdot (T_{wall,avg} - T_{fluid,avg}), \tag{6}$$

where Q is the absorbed heat in J, m is the mass of the water in kg, C_p is the specific heat capacity of water in $J/(kg \cdot K)$ and ΔT is the temperature difference in K between the inlet en outlet temperature of the water. In addition, h_c is the thermal conductivity coefficient in $W/(m^2 \cdot K)$, A_{cool} is the surface area of the cell in m^2, $T_{wall,avg}$ is the average temperature of the wall and $T_{fluid,avg}$ is the average temperature of the water in K. The details of these calculations are shown in Wien (2022).

2.5 Pressure increase

During the TR, moles of gas are released into the battery module or compartment. The free volume in this module or compartment remains constant, so pressure increases. To calculate the pressure increase as a result of the TR, the ideal gas law according Equation (7) is implemented:

$$P \cdot V = n \cdot R \cdot T, \tag{7}$$

where P is the pressure in Pa, V the volume in m^3, n the amount of moles, R the ideal gas constant equal to 8.314 $J/(mol \cdot K)$ and T the temperature in K. The pressure in the submarine, before the TR, will be assumed equal to

atmospheric pressure. With the volume and temperature of the room, the amount of moles before TR (n_{room}) can be calculated. The pressure increase (ΔP) will be established from the moles released during the TR (n_{TR}) and therefore the moles from the TR will be added to the moles already existing in the room before the TR. The gases released from the TR will have a higher temperature than the room temperature which results in the pressure and temperature increasing simultaneously. To calculate the pressure we first need to know the final temperature after the gases of the TR have mixed with the air. This can be calculated with Equation (8):

$$T_{final} = \frac{n_1 \cdot C_{v,1} \cdot T_1 + n_2 \cdot C_{v,2} \cdot T_2}{n_{final} \cdot C_{v,final}} \tag{8}$$

In this equation n_x is the amount of moles of gas, $C_{v,x}$ is the specific heat at constant volume in $\frac{kJ}{kg \cdot K}$ and T is the temperature in K. We can use this equation because we assume no work will be done when the gases are being mixed. To calculate the specific heat at constant volume we can use the values found by the model, displayed in Table 2 and combining those values with Equation (9):

$$C_{v,final} = \frac{n_1 \cdot C_{v,1} + n_2 \cdot C_{v,2}}{n_1 + n_2} \tag{9}$$

Using a constant volume and the newly calculated temperature of the room, the pressure increase can be established with Equation (10):

$$\Delta P = \frac{(n_{room} + n_{TR}) \cdot R \cdot T_{final}}{V_{room}} - P_{atm} \tag{10}$$

2.6 Model verification

To verify the used model we have to verify two components of the model. First the thermal model will be verified with the results of Feng et al. (2015) and secondly the gas model will be verified with the available literature. The results of the cooling model have been verified in Wien (2022), but are not explained in this paper because different cooling systems can be used to limit the impact of a TR and prevent cell-to-cell or module-to-module propagation.

2.6.1 Thermal model verification

In Feng et al. (2015) a model was built and verified with two experimental tests. Our used thermal model is based on their model and to verify whether the models compare, the different heat generation sources during the TR tests are compared. We show the heat generation of one test in Figure 3, as an example. The results shown are similar with the heat generation in Feng et al. (2015). The verification of the other tests are shown in Wien (2022) and we conclude that the thermal model is verified.

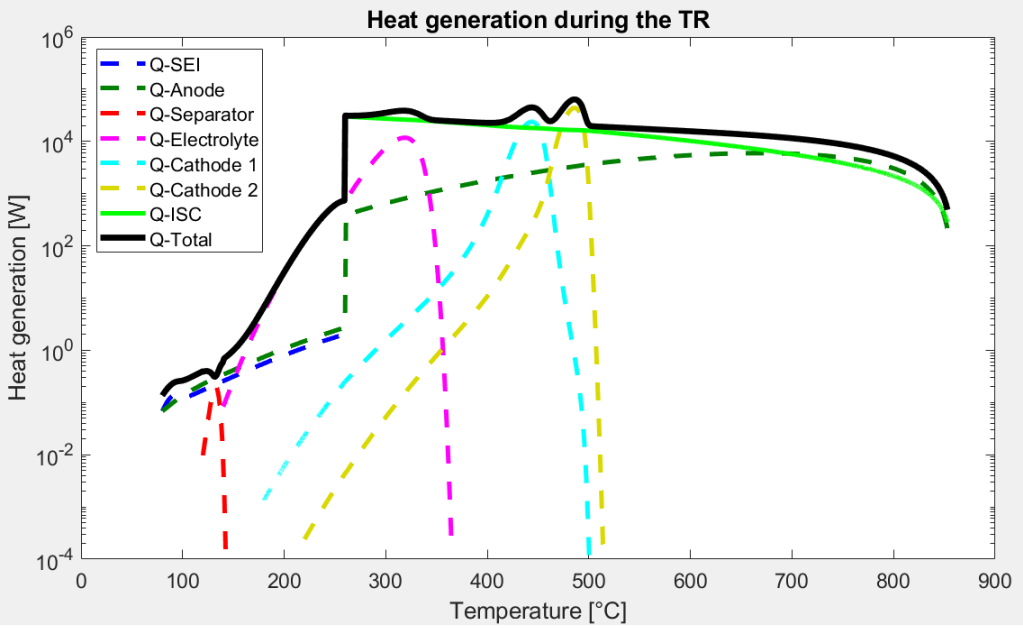

Figure 3: Heat generation during a TR from the used model.

2.6.2 Gas model verification

Koch et al. (2018) states that the amount of gas that is released during a TR can be determined relative to the capacity of the battery. They state that between 1.3 and 2.5 liters of gas is released per Ah and that there is a linear relationship between the amount of gas and the number of Ah, although in reality this will depend on the effectively used amount of material. The battery used in the model has a capacity of 25 Ah which results in 32.5 to 62.5 liters of gas. For an ideal gas, the volume for one mole of gas is equal to 24.465 liters at $T = 298\ K$ and $P = 1\ atm$. The amount of gas in mole should therefore be between $1.33 - 2.55$. The result of the model is that 2.18 mole is released which is within this range.

Beside the amount of gas, the distribution between the different type of gases has to be verified. Looking at experimental tests of a TR with NMC batteries, there is a wide percentage range between outcomes of different literature sources. In Table 2 those percentages and the outcome of the used model are displayed. As seen in the table, the percentages of the model match with the values found in experimental tests. However, because of the wide range, more research is needed to accurately verify the model and to establish what improvement is necessary.

Table 2: Experimentally measured percentages of different gases released during a TR of a NMC battery compared to percentages of the used model. Wien (2022)

Name of the gas	Chemical notation	Exp 1 %	Exp 2 %	Exp 3 %	Exp 4 %	Model %
Hydrogen	H_2	30.8	22.27	12.39	12.54	19.71
Carbon dioxide	CO_2	41.2	36.56	13.22	19.91	41.07
Carbon monoxide	CO	13.0	28.38	30.30	28.06	21.56
Methane	CH_4	6.8	5.26	10.50	12.90	7.64
Ethene	C_2H_4	8.2	5.61	0.10	0.16	6.19

3 Submarine battery system description

An initial battery system configuration for lithium-ion batteries for a notional future submarine is introduced in this section, based on current publicly available knowledge and inspired by the conceptual submarines under investigation in Stapersma and Prins (2020); Prins and Stapersma (2020).

3.1 Battery module

Since lithium-ion batteries for submarine propulsion are a relatively new concept, various modules have been analysed that have a sufficient TRL at the moment. The modules have been analysed in terms of cell energy density and module energy density, as can be seen in Table 3. Typical cell capacities vary between 48 and 200 Ah and cell energy densities vary between 357 and 417 Wh/L, whereas module energy densities vary between 107 and 246 Wh/L. Taking the dimensions and the amount of cells into account, a packing factor can be established, varying between 30% and 69%. For further calculations, a module packing factor of 69% will be considered, which is similar with the used value of 62.5% in De Vos et al. (2020).

3.2 Battery compartment

Typically, lithium-ion modules can be stacked into racks, which can be positioned in a battery compartment. The rack will have a specific packing factor and a lower energy density. First of all, a submarine lead-acid battery only consists of individual cells packed in a large battery compartment due to the large size of the individual cells. Lithium-ion cells are relatively much smaller and are therefore packed in modules and racks before placed in a battery compartment. The packing factors from cell to module ranges from 30% to 70% and from module to rack from 48% to 100%. This is strongly dependent on the form factor of the modules and rack construction and has a direct influence on heat management and thus the risk of thermal runaway. Therefore an average packing factor from module to rack of 56% is considered for further calculations based on the average between 64% and 48%.

The packing factors result in an energy density between 106.9 Wh/L and 149.9 Wh/L, two to three times as much as a lead-acid battery with an energy density of 54 Wh/L and a battery compartment packing factor of 51% (from Prins and Stapersma (2020)). However, the lead-acid packing factor of Prins and Stapersma (2020) takes into account the accessibility of the battery compartment. Accessibility is needed to be able to bridge any malfunctioning cells or perform maintenance applicable to the specific chemistry. The lithium-ion racks need to be accessible as well when placed in a compartment. When using an estimated packing factor of 65%, this would lead to an energy density between 69.5 Wh/L and 97.4 Wh/L, strongly reducing the original benefit of the high energy density of lithium-ion batteries. It is therefore important to maximise the packing factors of the modules and racks and minimise the maintenance space, if a significant improvement over lead-acid batteries is intended to be

realised. Future developments can potentially increase the energy density and packing factors as well. This would result in a different battery room layout, where for instance an access path between two modules can be created instead of a narrow access space above the cells, as is the case for traditional lead-acid battery rooms. However, the access path has to allow for maintenance and replacement of modules during the lifetime of the submarine. In conclusion, the energy density of the total system can potentially increase up to a factor 2, but only if sufficient packing density is achieved in a specific submarine design.

Table 3: Comparison of typical lithium-ion battery modules vs. lead-acid batteries.

Company Module	**Samsung** E3-M088	**EST-Floattech** Green Orca 1050	**Kokam** Kol Series	**Leclanché** M3 Energy	**MG Energy** RS Series	**Lead-Acid**
Cell						
Capacity [Ah]	94	200	103	60	48	11000
Energy density [Wh/L]	357,4	356,0	417,0	357,5	361,7	105,0
Module						
Capacity [kWh]	8,8	10,5	15,1	7,9	8,4	
Energy density [Wh/L]	233,4	106,9	155,8	246,5	123,5	
Packing factor [-]	62%	30%	38%	69%	34%	
Rack						
Energy density [Wh/L]	149,9	106,9		119,1		
Packing factor [-]	64%	100%		48%		
Compartment						
Energy density [Wh/L]	97,4	69,5		77,4		54
Packing factor [-]	65%	65%		65%		51%
Total packing factor [-]	40%	30%		33%		51%

3.3 Battery cooling

To prevent a temperature increase in the battery, the generated heat needs to be absorbed by a cooling system. During normal operation of the battery there are two types of cooling, which are air or liquid cooling. Liquid cooling has a higher heat transfer rate compared to air cooling, which results in a lower system volume to obtain the same cooling capacities. But liquid cooling has several disadvantages, such as potential leaks and the complex cooling techniques. Still, the amount of generated heat, especially during a TR, can realistically only be absorbed by the better cooling capacity of liquid. There are different ways to apply liquid cooling. As described in paragraph 2.4, pouch cells can be cooled by a water channel between individual cells, which can be used during a TR, but also during normal operation of the battery. Cooling during TR can alternatively be provided by fire extinguishing systems such as watermist and foam. In this paper cooling a battery in thermal runaway with foam will be analysed to identify what the cooling impact is on a TR.

3.4 Battery protection

The battery control and support system should consist of a number of defensive layers to prevent or limit the impact of thermal runaway: 1) Prevent initiation of a TR by a) cooling, b) cell level safety features and c) switching off cells by the BMS; 2) Prevent propagation of thermal runaway to neighbouring cells and modules by a) venting hot gasses and b) providing cooling with a fire extinguishing means; 3) Contain combustible gasses and heat to prevent further hazards to the crew.

Preventing the initiation of a thermal runaway (1) is not in scope of this study, although the thermal runaway and cooling models in this work can be used for evaluation of battery management control strategies. The main issue for the application of Li-ion batteries on submarines is that the combustible gasses and heat cannot be easily expanded to the environment. Therefore, in this work we investigate the feasibility of expanding the heat and gasses to the battery compartment and containing them in this compartment, while preventing further hazards by employing compressed air foam. The work intends to investigate the heat and gasses development and the effect of the added volume of compressed air foam, without providing full proof of the feasibility. Significant further experimental work will be required to validate the proposed approach.

4 Simulation experiments

4.1 Scenario

To analyse the impact of a TR on a submarine, different scenario's will be investigated. While surface vessels can eject the thermal runaway gasses, submarines have to contain the gasses when being submerged. Therefore, it is assumed in the following scenario's that the battery compartment will be airtight and designed to withstand pressure increases. Results will be shown for a TR in one single cell, in multiple cells and in one module, including the effects on the module and compartment pressures and the influence of cooling with compressed air foam.

For the scenario's we use a concept design of a notional future Diesel-Electric (DE) submarine, which is illustrated in Figure 4. It contains four LIB compartments (two on starboard side and two on port side). The batteries can be charged with the diesel generators (DG) and in case of a TR can be cooled with a fire extinguishing system (FE). The LIB compartments can be isolated to contain the gases released during a TR.

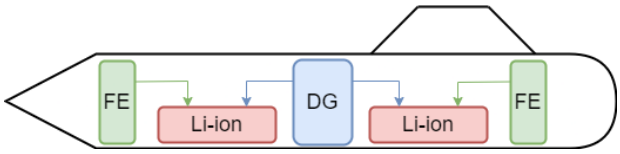

Figure 4: Schematic presentation of the DE-submarine.

4.2 Used battery system

The battery used in this scenario has a nominal voltage of 3.8 V and a capacity of 100 Ah. This will result in 380 Wh per LIB cell. The volume of the battery cell is 1.4 L which would result in an energy density of 271 Wh/L. This energy density cannot be achieved on a system level because we have to realise space for the modules and packs. To compensate the energy density a packing factor will be used of 0.69 for packing the cells into modules and 0.56 from module to rack. Implementing both factors results in a module energy density of 187 Wh/L and a compartment energy density of 105 Wh/L. For the capacity of the system, we assume the notional submarine in Prins and Stapersma (2020) and Stapersma and Prins (2020) with a battery capacity of approximately 5 MWh. For the Li-ion system we assume a doubled capacity due to the higher energy density. Therefore, a battery capacity of 10 MWh is assumed for a DE- submarine.

The assumed notional module will contain 25 battery cells. This will result in a module capacity of 9.5 kWh, which is similar with the module capacities in Table 3. Based on a module energy density of 187 Wh/L, a 9.5 kWh module will have a volume of 50.7 L. To calculate the amount of air in a module we assume that 69% of the volume is occupied by the battery cells and that 5% is used for cables and the battery management system. The rest of the modules consist of air which results in 13.2 L for each module. The four LIB compartments are used to realise the needed volume for a capacity of 10 MWh. Without exceeding the energy density of 105 Wh/L the total volume needed is 99 m^3. Each compartment will therefore have a volume of 24.75 m^3. If we assume that 56% of the compartment is used for the battery modules and an extra 5% is used for cables and module to module management, then a compartment contains 10.15 m^3 of air (excluding the air inside the modules).

4.3 Applied cooling containment method

The applied cooling and containment method in this scenario is compressed air foam. Compressed air foam uses water as a cooling substance, which is initially heated to 100 °C and subsequently evaporates. The foam ensures combustible gasses are contained without causing or expanding fire. We will use Equation (11) and (12) to establish the amount of heat water can absorb during liquid state and during vaporisation. After vaporisation it could be possible that the steam could increase in temperature and become superheated steam. However, it is assumed the steam will remain at 100 °C due to the significantly decreased heat capacity of steam. The gases from the TR and formed steam will increase the pressure in the module which will result in breaking of the pressure valve of the module. When this happens the steam will escape to the compartment and therefore has no time to extract further heat from the module.

$$Q_{water} = m \cdot C_{p,water} \cdot \Delta T_{water} \tag{11}$$

$$Q_{vap} = m \cdot \Delta H_{vap} \tag{12}$$

The used values for water are a specific heat capacity (C_p) of 4.2 $kJ/(kg \cdot K)$, a temperature increase (ΔT_{water}) from 25 °C to 100 °C and an enthaply of vaporisation (ΔH_{vap}) of 2256.4 kJ/kg. Combining these equations will result in Equation (13). With this equation the amount of water can be calculated to absorb all the heat from the TR during different scenarios.

$$Q_{cooling} = Q_{water} + Q_{vap} = m \cdot (C_{p,water} \cdot \Delta T + \Delta H_{vap}) = 2570.6 \cdot m \quad [kJ/kg] \tag{13}$$

The water will be injected into the module as compressed air foam. Compressed air foam will expand to 12 liter for every 1 liter of water used. Using nitrogen as the compressed gas this will prevent reactions with the released

gases during a TR. Applying compressed air foam will further increase the pressure in the compartment which can be calculated implementing the strategy in Section 2.5.

4.4 Results

Based on the battery modules and compartments described in section 4.2, various scenario's will be discussed and investigated, with increasing severity. First, the battery management system and the associated cooling system need to ensure the developed heat due to loading is dissipated to the cooling system and temperatures are maintained within safe limits. If an individual cell temperature rises above an unsafe threshold, the battery management system needs to switch off the specific cells or module. These two scenarios are not investigated in this work. When a cell enters into thermal runaway when the battery management system fails, for example due to a malfunction of a cell, the cell enters into thermal runaway and the model can be used to predict temperature development. In this first scenario, we will investigate whether cooling the cell with compressed air foam can theoretically stop or limit the effect of the TR, as demonstrated in Quintiere (2022) and Rao et al. (2015). Additionally, we analyse the pressure increase due to the TR gasses and compressed air foam. In the second scenario, we will assume a TR will take place completely in 1, 2 or 3 cells, investigating the effect of complete TR and cell-to-cell propagation and the impact of cooling with compressed air foam. Finally, we will investigate the scenario that the measures cannot prevent propagation within a module. These scenarios with increasing severity will provide guidance to the requirements and further validation of future battery management, cooling and firefighting systems.

In the first scenario, we investigate the initiation and development of a thermal runaway in a single cell, while applying cooling by the compressed foam system into the battery module from a certain activation temperature. The goal of adding a foam firefighting system is to prevent propagation of thermal runaway to adjacent cells and to contain both heat and combustible gasses, turning the foam into steam. When cooling is applied at an early stage, the thermal runaway might not fully develop and slow down or halt the reactions. After the initiation temperature of an ISC is reached, above 250 °C, the thermal runway cannot be stopped and all heat and gasses will develop, as illustrated in Figure 3. In Figure 5, the required volume of water and nitrogen (components of the foam) are presented to cool a TR at various activation temperatures between 100°C and 300°C. Additionally, the pressure increase is displayed due to the released TR gasses, the added volume of water and nitrogen and the increase in volume due to the formation of steam. The maximum added volume of foam is 11.5 L, which can fit in the free volume of the module (13.2 L). However, the amount of foam needed to dissipate the heat of a fully developed TR results in an pressure increase up to 60 bar, thus addresses the need of a pressure release valve since pressures are extremely high to contain within the module. Concluding, the theoretical model demonstrates that cooling that is initiated sufficiently before an ISC at 250°C can limit the effect of a thermal runaway, a result which should clearly be validated in future work.

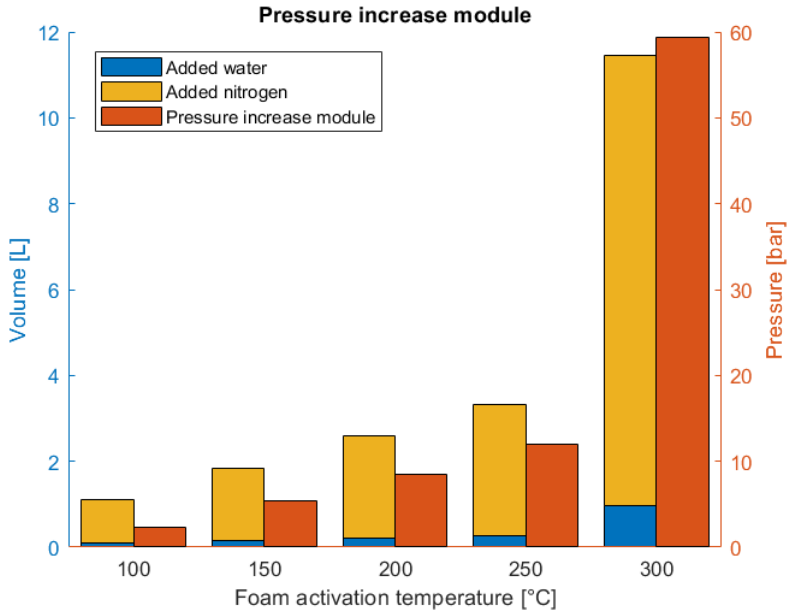

Figure 5: Pressure increase when a TR happens at 1 cell within a module.

In the second scenario, a thermal runaway of one, two and three cells will be investigated by applying cooling with a compressed foam system while containing all gasses in the battery compartment instead of the module.

Additionally, a comparison is made when the compressed foam system is not activated. According to the ideal gas law and equations 8, 9 and 10, the pressure increase has been established. The results are shown in Figure 6. Looking at Figure 6a, it can be seen that the pressures in the compartment remain significantly lower compared to scenario 1, where all gasses were contained within the module, due to the larger free volume. The pressure increase remains below 0.8 bar, even if multiple cells develop a complete thermal runaway. If the compressed foam system is initiated at lower temperatures, the pressure increase is further reduced to 0.2 bar. The compartment design should therefore be engineered such that the estimated pressures can be resisted. If we however assume the same TR scenario without the addition of the compressed air foam, we see that the maximum pressures are further reduced to a maximum of 0.3 bar (Figure 6b). This could be realised by an intrinsically safe module design that potentially limits TR propagation to three cells. However, it has to be taken into account that the gasses ejected into the compartment have much higher temperatures, thus causing different risks. In conclusion, when a cell enters into thermal runaway, the pressure build-up needs to be vented to the compartment, which leads to an acceptable pressure increase if TR is limited to 3 cells, while significant amounts of heat and combustible gasses cause a dangerous hazard in the battery compartment.

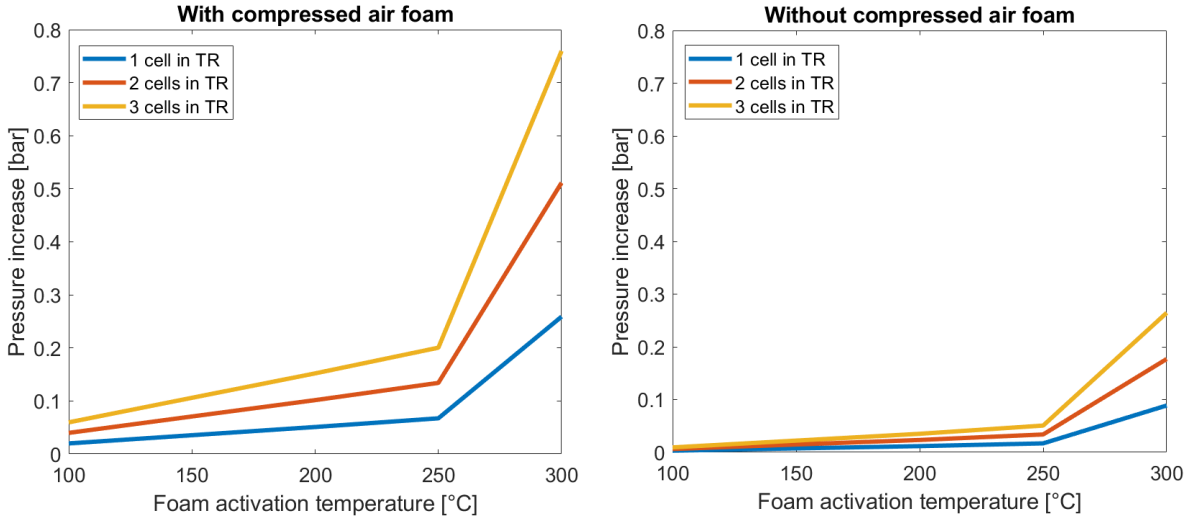

(a) With compressed air foam

(b) Without compressed air foam

Figure 6: Pressure increase when a number of cells go into TR depending on the foam activation temperatures.

In the third and final scenario, we will look at the pressure increase as a result of a TR ranging from one cell up to the entire module (25 cells). We will look only at the pressure increase as a result of the gases from the TR on a compartment. As demonstrated in Figure 7, the pressure increases linearly with the amount of cells that go into thermal runaway. If all cells in a module develop a TR, the compartment pressure increases with more than two bars of pressure. In the figure, the dashed lines indicate the pressure increase of one, two or three cells that have been suppressed by the compressed foam system. From this we can conclude that 9 cells can go into TR before reaching the equivalent pressure of three cells in TR that have been cooled with foam. However, without suppression the compartment will be filled with hot and combustible gasses, which poses a serious risk of explosion or fire. This demonstrates that any design of a battery systems should prevent cell-to-cell propagation and thermal runaway of all or most cells in a module as the effect of TR of a complete module cannot be safely contained in a battery compartment.

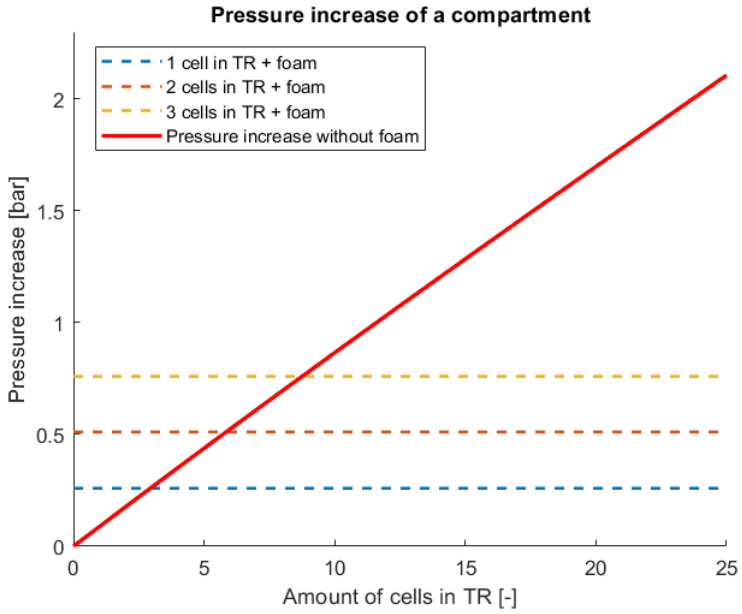

Figure 7: Pressure increase of a compartment when a percentage of cells go into TR with and without air foam cooling.

5 Conclusions and further research

In this paper, the approach of combining two thermal runaway models has been proposed for evaluation of lithium-ion battery and associated cooling and fire suppression system design. Both heat generation and gas generation of a thermal runaway process can be established with the proposed approach, as well as the effect of simultaneous cooling either by a cooling system or by a firefighting system. A case study has been performed to analyse the effects on a notional submarine battery module and compartment in terms of the risk of propagation of thermal runaway to other cells, the effect of venting into the compartment and cooling by a compressed air foam system and the resulting pressure increase in the closed battery compartment. In addition to this, the influence of a compressed air foam extinguishing medium in TR mitigation and containment has been discussed.

The case study results have demonstrated that pressures can increase up to 60 bars in a module if the gasses developed during TR are contained in the battery module. This confirms the need of a pressure release valve, to allow the pressure to be dispersed in the battery compartment. This results in considerations that have to be made regarding the number of compartments. More compartments have the advantage that a smaller percentage of battery capacity is lost due to a failure or thermal runaway in one of the compartments. On the other hand, more compartments lower the volume of air in each compartment, having the consequence that a lower free volume of air results in a higher compartment pressure during a thermal runaway event of a single cell. In this study, we have investigated a configuration with four battery compartments, which leads to a 25% reduction in capacity due to the loss of a battery compartment.

To prevent high pressures in the compartment, it is essential to contain the thermal runaway to one or a small amount of cells and prevent further propagation to surrounding cells (and modules). Passive TR propagation prevention is therefore desired on a cell level. The results of the proposed models indicate that thermal runaway can be stopped if foam is activated at an early stage of TR development and can dissipate the heat of a fully developed TR in order to prevent cell-to-cell propagation. However, the addition of the foam and transition into steam results in an undesired pressure increase. Therefore, the combination of the three defensive layers to 1) prevent initiation of a TR, 2) prevent propagation of a TR and 3) contain combustible gasses and heat to prevent further hazards to the crew should be implemented to reduce the TR consequences. The proposed approach can be used to analyse the desired initiation moment and impact of the three defensive measures.

The modelling approach in this work can be further improved by investigating the assumptions underpinning the proposed approach (Wien, 2022). First, the chemical reactions taking place during the decomposition of the electrolyte are not yet accurately determined. Further research is needed to establish which substances are released during the reactions and which substances react. It is not only necessary to look at different organic solutions individually, but also the combination of these substances and the impact on the TR. Secondly, this model looks at a single cell going into TR without taking into account the impact of surrounding cells. In order to secure a complete module, it will also be necessary to look at the propagation between different cells more accurately and investigate how heat is transferred from one cell to another. Third, the model assumes that the temperature of the

cell is uniformly distributed and that all heat is generated equally. In reality a temperature gradient exits between the walls and the center of the battery and the side of the anode could be hotter than the side of the cathode. These differences can influence the results and it is therefore important that research is carried out into the spatial temperature development inside the battery cell. With these extensions, increased fidelity and accuracy of the proposed approach can be achieved.

While the modelling approach has been verified against standard tests from literature, verification and validation of modelling results for the investigated scenarios is required to increase confidence in this study's results. For this validation, tests for a specific battery system and associated cooling and firefighting system is required. Moreover, the cooling model could be extended to include the effect of steam formation on the effectiveness of compressed air foam. Moreover, extensive further design and testing is required to design a battery system that reduces the probability of thermal runaway propagation from cell-to-cell to an acceptable level. If the risk of thermal runaway can thus be sufficiently mitigated and the battery packing factor can be kept sufficiently high, then Li-ion batteries can double the range of future submarines.

References

Chombo, P.V., Laoonual, Y., 2020. A review of safety strategies of a li-ion battery. Journal of Power Sources 478, 228649.

De Vos, P., Los, S.A., Ten Hacken, M., Rietveld, L.P.W., Schiks, W., Boogaart, R., Visser, K., Hopman, J.J., 2020. Innovative, non-nuclear Power Plant Concepts for modern Submarines with very low Indiscretion Ratio .

Feng, X., He, X., Ouyang, M., Lu, L., Wu, P., Kulp, C., Prasser, S., 2015. Thermal runaway propagation model for designing a safer battery pack with 25 ah $LiNi_xCo_yMn_zO_2$ large format lithium ion battery. Applied Energy 154, 74–91.

Gartner, N.H.D., 2021. Thermal behaviour of lithium-ion batteries and the implications on submarine design. MSc. thesis Delft University of Technology .

Geertsma, R.D., Negenborn, R.R., Visser, K., Hopman, J.J., 2017. Design and control of hybrid power and propulsion systems for smart ships: a review of developments. Applied Energy 194, 30–54.

Golubkov, A.W., Fuchs, D., Wagner, J., Wiltsche, H., Stangl, C., Fauler, G., Voitic, G., Thaler, A., Hacker, V., 2014. Thermal-runaway experiments on consumer li-ion batteries with metal-oxide and olivin-type cathodes. RSC Advances 4, 3633.

Koch, S., Fill, A., Birke, K.P., 2018. Comprehensive gas analysis on large scale automotive lithium-ion cells in thermal runaway. Journal of Power Sources 398, 106–122.

Lai, X., Jin, C., Yi, W., Han, X., Feng, X., Zheng, Y., Ouyang, M., 2021. Mechanism, modelling, detection, and prevention of the internal short circuit in lithium-ion batteries: recent advances and perspectives. Energy Storage Materials 35, 470–499.

Netherlands Ministry of Defence, 2012. Summary Defence White paper 2022: A stronger Netherlands, a safer Europe, investing in a robust NATO and EU .

Pilat, T., Grzegorz, G., Polak, A., Kurys, P., 2017. Implementation of the assessment method of the lead-acid battery electrical capacity of submarines. Journal of Marine Engineering and Technology 16:4, 326–330.

Prins, C., Stapersma, D., 2020. Aip for ocean going submarines: off-the-shelf or promise .

Quintiere, J.G., 2022. On a method to mitigate thermal runaway and propagation in packages of lithium ion batteries 130, 103573.

Rao, H., Huang, Z., Zhang, H., Xiao, S., 2015. Study of fire tests and fire safety measures on lithium-ion battery used on ships .

Stapersma, D., Prins, C., 2020. The importance of submarine air-independent power for operational agility .

Wien, T.H., 2022. Thermal runaway bij lithium-ion batterijen: Onderzoek naar de ontwikkeling van warmte en gassen tijdens een thermal runaway .